Article

SOURCE DATA | TRANSPARENT PROCESS

THE EMBO JOURNAL

Suppression of miR-199a maturation by HuR is crucial for hypoxia-induced glycolytic switch in hepatocellular carcinoma

Ling-Fei Zhang[1,2], Jia-Tao Lou[3], Ming-Hua Lu[1,2], Chunfang Gao[4], Shuang Zhao[1,2], Biao Li[5], Sheng Liang[6], Yong Li[7], Dangsheng Li[8] & Mo-Fang Liu[1,2,*]

Abstract

Glucose metabolic reprogramming is a hallmark of cancer. Cancer cells rapidly adjust their energy source from oxidative phosphorylation to glycolytic metabolism in order to efficiently proliferate in a hypoxic environment, but the mechanism underlying this switch is still incompletely understood. Here, we report that hypoxia potently induces the RNA-binding protein HuR to specifically bind primary miR-199a transcript to block miR-199a maturation in hepatocellular carcinoma (HCC) cells. We demonstrate that this hypoxia-suppressed miR-199a plays a decisive role in limiting glycolysis in HCC cells by targeting hexokinase-2 (*Hk2*) and pyruvate kinase-M2 (*Pkm2*). Furthermore, systemically delivered cholesterol-modified agomiR-199a inhibits [^{18}F]-fluorodeoxyglucose uptake and attenuates tumor growth in HCC tumor-bearing mice. These data reveal a novel mechanism of reprogramming of cancer energy metabolism in which HuR suppresses miR-199a maturation to link hypoxia to the Warburg effect and suggest a promising therapeutic strategy that targets miR-199a to interrupt cancerous aerobic glycolysis.

Keywords glycolysis; hepatocellular carcinoma; HK2 and PKM2; hypoxia; miR-199a

Subject Categories Cancer; Metabolism; RNA Biology

DOI 10.15252/embj.201591803 | Received 15 April 2015 | Revised 11 August 2015 | Accepted 20 August 2015 | Published online 7 September 2015

The EMBO Journal (2015) 34: 2671–2685

Introduction

Hypoxia, one of the most prevalent and fundamentally important features of solid tumors, contributes to the reprogramming of cancer metabolism from oxidative to glycolytic metabolism in cancer cells, thus maintaining redox homeostasis and cell survival under conditions of prolonged hypoxia (Airley & Mobasheri, 2007; Wilson & Hay, 2011). This anomalous characteristic of glucose metabolism in cancer cells, known as the Warburg effect, leads to increased glucose uptake, accelerated glycolysis, and lactate production (Warburg, 1956). [^{18}F]-Fluorodeoxyglucose ([^{18}F]FDG) positron emission tomography combined with computer tomography (PET/CT) imaging effectively detects malignant tumors because it takes advantage of the increased glucose uptake by cancer cells (Di Chiro *et al*, 1982; Mankoff *et al*, 2007). Moreover, the Warburg effect also confers advantages to tumor growth (Kroemer & Pouyssegur, 2008; Vander Heiden *et al*, 2009) and provides conditions favoring tumor invasion and metastasis (Swietach *et al*, 2007) and suppression of anticancer immune effectors (Fischer *et al*, 2007). Hexokinase 2 (HK2) and pyruvate kinase M2 (PKM2) are, respectively, the major hexokinase and pyruvate kinase isozymes in tumors and have been documented as pivotal players in the Warburg effect and utilized as metabolic targets in developing new antitumor agents (Mathupala *et al*, 2009; Vander Heiden, 2011; Luo & Semenza, 2012).

Previous studies have advanced our understanding of the mechanisms underlying hypoxia-induced cellular responses in cancer cells (Majmundar *et al*, 2010). In particular, transcription of several glycolytic genes vital to the Warburg effect (including *Hk2* and *Pkm2*) has been shown to be activated by hypoxia-inducible factor-1 (HIF-1), an oxygen-sensitive transcription factor (Semenza, 2010). miRNAs are an emerging class of gene

1 Center for RNA Research, State Key Laboratory of Molecular Biology–University of Chinese Academy of Sciences, Institute of Biochemistry and Cell Biology, Shanghai Institutes for Biological Sciences, Chinese Academy of Sciences, Shanghai, China
2 Shanghai Key Laboratory of Molecular Andrology, Institute of Biochemistry and Cell Biology, Shanghai Institutes for Biological Sciences, Chinese Academy of Sciences, Shanghai, China
3 Department of Laboratory Medicine, Shanghai Chest Hospital, Shanghai Jiao Tong University, Shanghai, China
4 Department of Laboratory Medicine, Eastern Hepatobiliary Surgical Hospital, Second Military Medical University, Shanghai, China
5 Department of Nuclear Medicine and Micro PET Center, Rui Jin Hospital Affiliated to Shanghai Jiao Tong University School of Medicine, Shanghai, China
6 Department of Nuclear Medicine, Xin Hua Hospital Affiliated to Shanghai Jiao Tong University School of Medicine, Shanghai, China
7 Department of Cancer Biology, Lerner Research Institute, Cleveland Clinic, Cleveland, OH, USA
8 Shanghai Information Center for Life Sciences, Shanghai Institutes for Biological Sciences, Chinese Academy of Sciences, Shanghai, China
*Corresponding author. Tel: +86 21 54921146; Fax: +86 21 54921011; E-mail: mfliu@sibcb.ac.cn

regulators that negatively regulate gene expression at the post-transcriptional level (Wu & Belasco, 2008) and are involved in virtually all physiological and pathological processes (Guarnieri & DiLeone, 2008). However, whether and how miRNAs are involved in regulating the glycolytic switch under hypoxia in cancer cells remains largely unexplored.

In the present study, we found that repression of miR-199a by hypoxia is crucial for hypoxic stress to accelerate glycolysis in hepatocellular carcinoma (HCC) cells. Mechanistically, hypoxic stress in HCC cells promotes the binding of RNA-binding protein HuR to the primary transcript of miR-199a (pri-miR-199a), blocking its processing into mature miR-199a. Our results showed that miR-199a inhibited glycolysis in cultured HCC cells and decreased [^{18}F]FDG uptake in HCC tumors. Interestingly, we identified *Hk2* and *Pkm2* as novel targets of miR-199a and revealed that miR-199a suppressed glycolysis in HCC cells by negatively regulating these two key glycolytic genes. Importantly, systemic delivery of a miR-199a agonist to mice bearing HCC subcutaneous tumors markedly reduced both tumor growth and [^{18}F]FDG uptake. Collectively, our findings indicate that miR-199a is a robust inhibitor of the Warburg effect and a promising therapeutic target for HCC treatment, adding a new dimension to hypoxia-mediated regulation of cancer metabolism.

Results

Down-regulation of *mir-199a* is crucial for the glycolysis-promoting effect of hypoxia in human HCC cells

To gain new insights into hypoxia-mediated regulation of cancer metabolism, using qRT–PCR, we compared the expression of 38 cancer-related miRNAs (Garzon *et al*, 2010; Liu *et al*, 2010) in the human HCC cell lines SMMC-7721 and Hep3B with and without hypoxia induction. Six miRNAs (miR-155, miR-210, miR-203, miR-221, miR-15a, and miR-125b) were commonly up-regulated in both HCC cell lines during hypoxia (Fig 1A). Among these, *mir-155* was the most markedly up-regulated by hypoxia, consistent with a previous observation in lung cancer cells (Babar *et al*, 2011). Intriguingly, hypoxia treatment also led to a common down-regulation of 5 miRNAs (miR-199a, miR-34a, miR-301, miR-181a, and miR-181c) in both cell lines. miR-199a, among all the tested miRNAs, had the greatest reduction in both hypoxia-treated cell lines (Fig 1A), implicating repression of *mir-199a* as a potentially important mechanism underlying hypoxia-induced cellular responses.

We next examined whether down-regulation of *mir-199a* is involved in the metabolic response to hypoxia in human HCC cells. As expected, we found that hypoxic stress substantially increased the rates of glucose consumption and lactate production in HCC cells (Fig 1B and C). Intriguingly, restoration of *mir-199a* expression by transfection of miR-199a mimics at a dosage as low as 0.5 nmol/l completely reversed the impact of hypoxic stress on glucose consumption and lactate production in both Hep3B and SMMC-7721 cells (Fig 1B and C; Appendix Fig S1). These results together suggest that down-regulation of *mir-199a* represents an important mechanism for the glycolysis-promoting effect of hypoxia in HCC cells.

Hypoxia selectively inhibits the processing of pri-miR-199a in human HCC cells

We next asked how hypoxia down-regulates *mir-199a* in human HCC cells. In the human genome, miR-199a is encoded at two loci, *mir-199a-1* and *mir-199a-2*. Intriguingly, the pri-miR-199a-2 level was much higher than that of pri-miR-199a-1 in both SMMC-7721 and Hep3B cells, suggesting that *mir-199a-2* is the major source of miR-199a expression in HCC cells (Appendix Fig S2A). We thus decided to investigate the regulation of *mir-199a-2* in HCC cells. *mir-199a-2*, together with *mir-214*, is located within a long noncoding RNA, DNM3os, in which the binding sites for Drosha are proximal to the upstream and downstream of two pre-miRNA sequences (Fukuda *et al*, 2007; Lee *et al*, 2009; Fig 2A). We found that *DNM3os* in Hep3B and SMMC-7721 cells was significantly up-regulated by hypoxia (Fig 2B and Appendix Fig S2B). This perhaps comes as no surprise given a previous study showing that Twist-1, a transcriptional activator for *DNM3os* (Lee *et al*, 2009), is activated by HIF-1 (Sun *et al*, 2009). Indeed, Twist-1 was up-regulated in hypoxic HCC cells (Appendix Fig S2C). Consistently, the level of miR-214, the other miRNA encoded in *DNM3os*, also was modestly increased along with *DNM3os* expression in hypoxic HCC cells, despite reduction in the levels of miR-199a and its partner miR-199a* (Fig 2B and Appendix Fig S2B). These results suggest that hypoxia likely selectively inhibited the processing of miR-199a in HCC cells.

We next asked at which step miR-199a processing is inhibited in hypoxic HCC cells. Northern blot analysis showed that both mature and precursor forms of miR-199a were significantly reduced with a concomitant increase of pri-miR-199a in hypoxic Hep3B cells compared with that in normoxic cells (Fig 2C). In sharp contrast, the primary form of miR-214 was barely detected in hypoxic Hep 3B cells by Northern blot (Appendix Fig S2D, lane 6), suggesting that this miRNA is rapidly processed in these cells whereas pri-miR-199a is not. These results strongly suggest that miR-199a expression is blocked at the pri-miRNA processing step under hypoxic conditions. To further corroborate this, we constructed a *pri-mir-199a/214* expression vector, containing the H1 promoter-driven *mir-199a-2* (~1 kb) and *mir-214* sequences (~2 kb) (as shown in Fig 2A, bottom). Transfecting this vector into Hep3B cells led to about a threefold increase of mature miR-199a compared with control vector, but under hypoxia this increase was strongly attenuated (Fig 2D, left). In sharp contrast, in synthetic pre-miR-199a-transfected cells, the increase of mature miR-199a was no longer modulated by hypoxia treatment, indicating that the processing step by Dicer is not disturbed by hypoxia. Of note, transfection of the *pri-mir-199a/214* vector also resulted in about a fourfold increase of miR-214, while this increase was not modulated by hypoxia stress (Fig 2D, right). These results together indicate that hypoxia selectively inhibits pri-miR-199a processing in human HCC cells.

Hypoxia enhances HuR binding to pri-miR-199a and consequently represses its processing in human HCC cells

We next asked how hypoxia inhibits pri-miR-199a processing. The expression of Drosha and DGCR8, two key components of the microprocessor, was unaltered in hypoxic cells (Appendix Fig S2E).

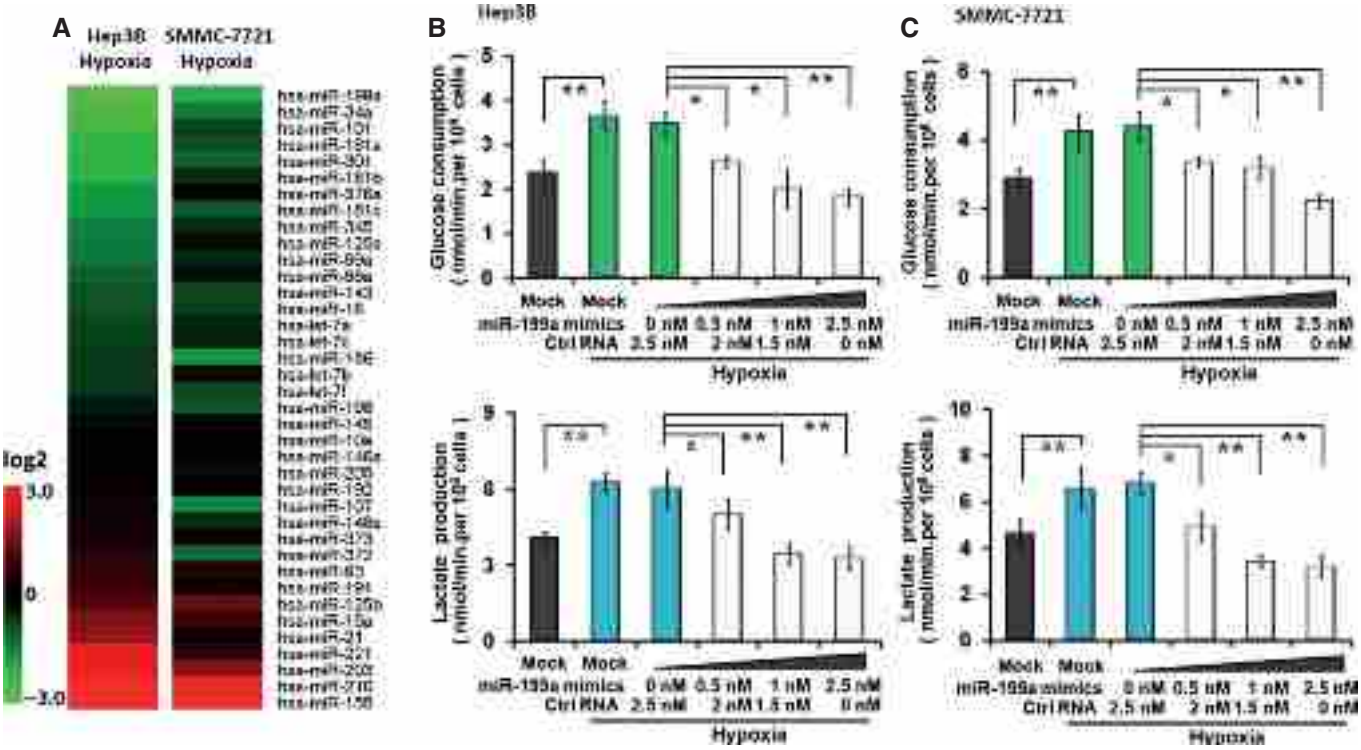

Figure 1. Hypoxia promotes glucose metabolism in hepatocellular carcinoma (HCC) cells through down-regulating *mir-199a*.

A The effect of hypoxia on expression of 38 cancer-related miRNAs in HCC cell lines Hep3B and SMMC-7721. The heatmap represents differentially expressed miRNAs at 24 h post-hypoxia treatment, with the up-regulated miRNAs in red and down-regulated ones in green.

B, C Restoration of *mir-199a* expression overrode the glycolysis-promoting effect of hypoxia in Hep3B (B) and SMMC-7721 cells (C). The average values ± SD of three separate experiments are plotted. Statistics: Student's *t*-test; $*P < 0.05$, $**P < 0.01$.

Notably, several microprocessor inhibitors, including Lin28 (Viswanathan *et al*, 2008), NF90-NF45 (Sakamoto *et al*, 2009), MSI2 and HuR (Choudhury *et al*, 2013), and YAP (Mori *et al*, 2014), have been reported to repress the processing of distinct subsets of pri-miRNAs by binding to their specific sequence motifs. We thus knocked down these microprocessor inhibitors in HCC cells (Appendix Fig S2F) and found that depletion of HuR, but not Lin28, NF90-NF45, MSI2, or YAP, completely overrode the repressive effect of hypoxia on miR-199a expression in both Hep3B and SMMC-7721 cells (Fig 2E and Appendix Fig S2G), indicating that HuR is required for hypoxia-mediated blockade of pri-miR-199a processing.

Interestingly, by searching for HuR-binding motifs (Ray *et al*, 2009) in human DNM3os transcript, we found 4 putative HuR-binding motifs juxtaposed to pre-miR-199a, but none near pre-miR-214 sequences (Fig 2A). Importantly, our RNA immunoprecipitation combined with qRT–PCR showed that pri-miR-199a was significantly enriched by antibodies against HuR compared to IgG control, and this enrichment was greatly increased in hypoxic HCC cells (Fig 2F and Appendix Fig S2H). In contrast, pri-miR-214, as well as negative control GAPDH mRNA, was barely detected in anti-HuR immunoprecipitates in either normoxic or hypoxic cells. These results together support that hypoxia potentiates the binding of HuR to pri-miR-199a in HCC cells.

We next asked whether binding of HuR is essential for hypoxia-mediated blockade of pri-miR-199a processing. To this end, we generated two HuR-binding mutants by deleting two sites juxtaposed to the upstream and downstream ends of pre-miR-199a sequences (Mut-1) or two sites at ~300 nt downstream of pre-miR-199a (Mut-2) in the *pri-mir-199a/214* expression vector (Fig 2G, top). Electrophoresis mobility assays showed that both Mut-1 and Mut-2 transcripts had a severely compromised ability to bind HuR (Appendix Fig S2I). Interestingly, transfection of the mutated vectors into Hep3B cells led to an increase of mature miR-199a similar to that in wild-type expression vector, but miR-199a overexpression in the mutated vector-transfected cells was no longer attenuated by hypoxia or modulated by HuR knockdown (Fig 2G), supporting the idea that HuR binding is critical for hypoxia-mediated inhibition of pri-miR-199a processing. In contrast, either *HuR* knockdown or depletion of HuR-binding sites in the expression vector had little impact on miR-214 overexpression in transfected cells (Appendix Fig S2J). Collectively, these results suggest that hypoxia promotes HuR binding to pri-miR-199a and consequently inhibits its processing in human HCC cells.

Additionally, *HuR* knockdown effectively attenuated the stimulatory impact of hypoxia on glucose metabolism in Hep3B cells, whereas inhibition of miR-199a function by anti-miR-199a partially restored the glucose consumption and lactate production rates (Appendix Fig S3A). This is consistent with our above finding that *mir-199a* down-regulation has an essential role in the glycolysis-promoting effect of hypoxia (Fig 1), strongly supporting our hypothesis that the HuR:miR-199a axis is critical to regulating the

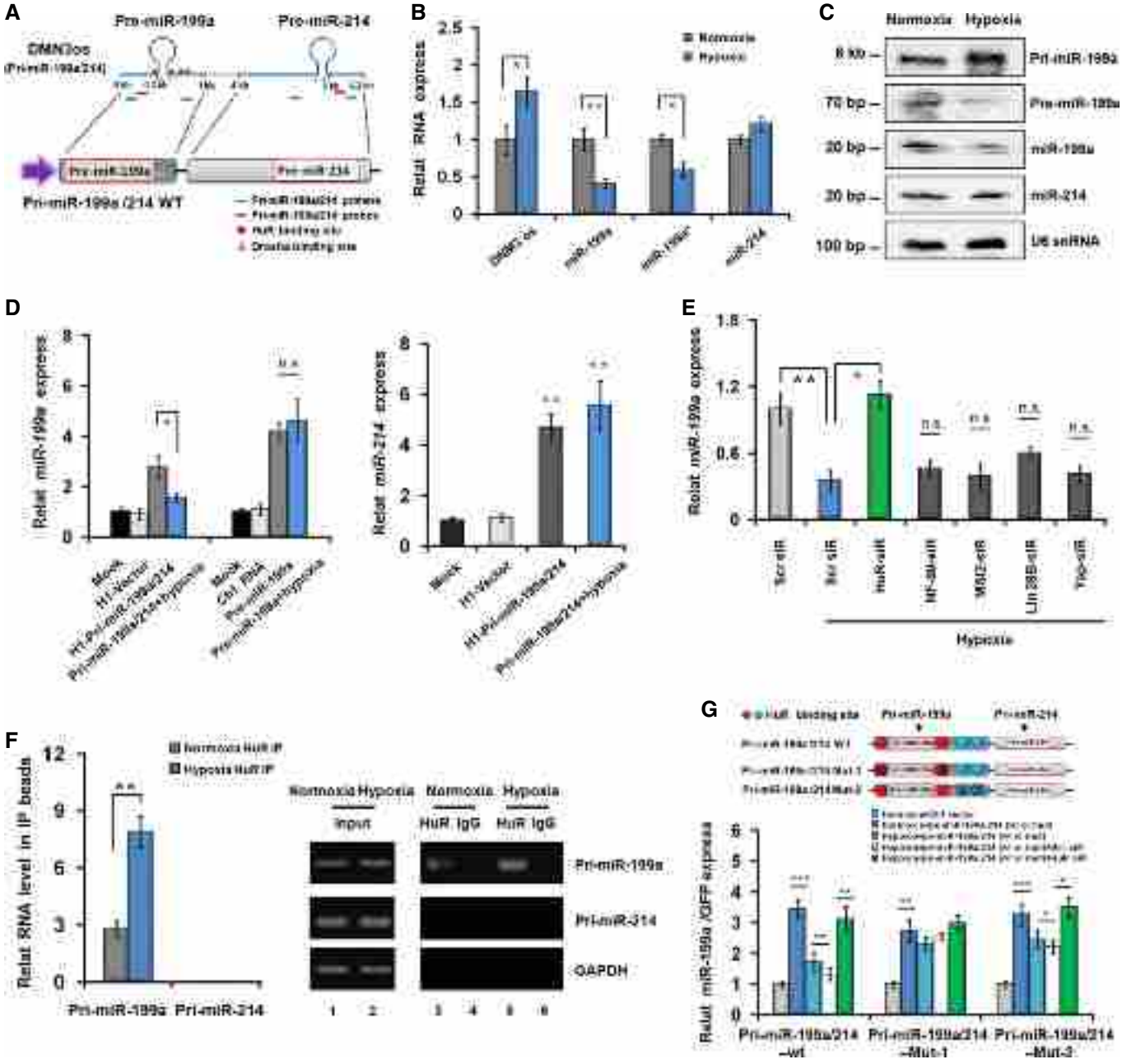

Figure 2. Hypoxia promotes HuR binding to pri-miR-199a and blocks miR-199a maturation in HCC cells.

A Schematic representation of the DNM3os (miR-199a/214 cluster) transcript (top) and construction of pri-miR-199a/214 expression vector (bottom). The qRT–PCR primer sets, Northern blot probes, predicted HuR-binding sites, and Drosha binding sites are indicated in DNM3os (top).

B qRT–PCR analyses of DNM3os, miR-199a, miR-199a*, or miR-214 expression in Hep3B cells under normoxic or hypoxic conditions.

C Northern blot assays of miR-199a processing in Hep3B cells under normoxic or hypoxic conditions.

D qRT–PCR analyses of miR-199a and miR-214 levels in pri-miR-199a/214 vector- or synthesized pre-miR-199a-transfected Hep3B cells under normoxic or hypoxic conditions.

E RNAi knockdown of *HuR*, but not other indicated factors, completely restored miR-199a expression in hypoxic Hep3B cells. The cells were transfected with the indicated siRNAs for *HuR*, *NF90*, *MSI2*, *Lin28*, or *YAP*, with scrambled siRNA (Scr siR) serving as a negative control.

F RNA immunoprecipitation combined with qRT–PCR assays of HuR binding to pri-miR-199a or pri-miR-214 in normoxic or hypoxic Hep3B cells. Left, relative enrichment of pri-miRNAs in HuR IP compared with IgG IP and normalized to negative control GAPDH mRNA level in IP beads; right, visualization of qRT–PCR products using ethidium bromide-stained agarose gels.

G qRT–PCR analyses of miR-199a levels in wild-type or HuR-binding-site-mutated pri-miR-199a/214 vector (Mut-1 or Mut-2)-transfected Hep3B cells under indicated conditions.

Data information: The average values ± SD of three separate experiments are plotted. Statistics: Student's *t*-test; $*P < 0.05$, $**P < 0.01$, $***P < 0.001$.
Source data are available online for this figure.

glycolytic switch under hypoxia. Moreover, *HuR* knockdown significantly reduced cell proliferation and transwell migration in Hep3B cells cultured under hypoxia condition as well as the rate of Hep3B tumor growth in nude mice, while transfection of anti-miR-199a effectively restored HCC tumorigenesis *in vitro* and *in vivo* (Appendix Fig S3B). These results together suggest that hypoxia-induced suppression of miR-199a maturation by HuR is important for both glucose metabolism and tumorigenesis in human HCC cells.

miR-199a directly targets *Hk2* and *Pkm2*

Our above results suggest miR-199a suppresses hypoxia-induced glycolysis in HCC cells (Fig 1). We next explored how miR-199a achieves this in HCC cells. Interestingly, using computational prediction programs (Krek *et al*, 2005; Lewis *et al*, 2005), we found that *Hk2* and *Pkm2*, two key glycolytic genes in the Warburg effect (Mathupala *et al*, 2009; Luo & Semenza, 2012), were predicted to be targets of miR-199a (Fig 3A, top). To experimentally test whether

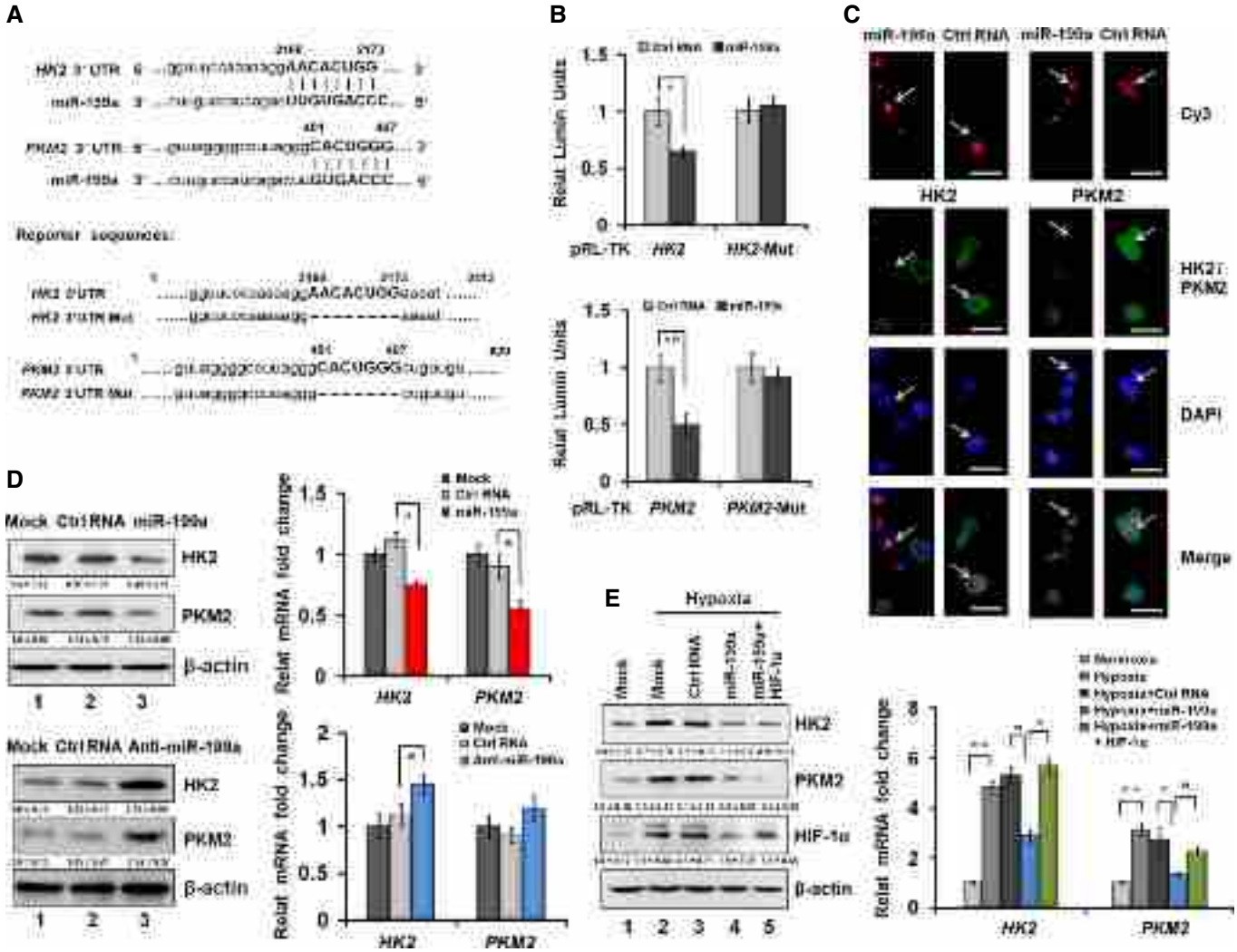

Figure 3. *Hk2* and *Pkm2* are suppressed by miR-199a in HCC cells.

A *Hk2* and *Pkm2* were predicted as miR-199a targets. Top, predicted miR-199a regulatory elements (seed sequences in upper case) in the *Hk2* and *Pkm2* 3′ UTRs; bottom, sequences of wild-type (pRL-*HK2* 3′ UTR, pRL-*PKM2* 3′ UTR) and mutated 3′ UTR-*Renilla* luciferase reporters (pRL-*HK2* 3′ UTR Mut, pRL-*PKM2* 3′ UTR Mut).

B Luciferase reporter assays. *Renilla* luciferase activity (relative luminescence); Ctrl RNA was set to 1.0 in each experiment, and the luciferase activity for each miR-199a mimic was normalized relative to its respective control.

C Immunofluorescence analyses of endogenous HK2 and PKM2 protein expression (green) in Cy3-labeled miR-199a mimic- or Ctrl RNA-transfected SMMC-7721 cells (red). Nuclei were counterstained with DAPI (blue). Scale bar, 50 μm.

D Western blot (left) or qRT–PCR analyses (right) of *Hk2* and *Pkm2* expression in miR-199a mimic- (top) or anti-miR-199a-transfected Hep3B cells (bottom).

E miR-199a repressed transcription of *Hk2* and *Pkm2* in hypoxic HCC cells via targeting *HIF1α*. Western blot of HK2, PKM2, and HIF1α protein levels (left) and qRT–PCR analyses of *Hk2* and *Pkm2* mRNA levels in Hep3B cells (right) were performed under indicated conditions.

Data information: The average values ± SD of three separate experiments are plotted. The relative levels of HK2, PKM2, and HIF-1α proteins are indicated in (D) and (E) (the one in mock is set as 1.0). Statistics: Student's *t*-test; $*P < 0.05$, $**P < 0.01$.
Source data are available online for this figure.

miR-199a regulates *Hk2* and *Pkm2*, we constructed luciferase reporters by cloning the wild-type 3′ UTRs of *Hk2* and *Pkm2* or their mutant versions downstream of the *Renilla* luciferase cDNA in the pRL-TK vector (Fig 3A, bottom). We found that co-transfection of miR-199a mimics significantly decreased luciferase activity of the reporters in the wild-type but barely affected the reporters in the mutants (Fig 3B), suggesting that *Hk2* and *Pkm2* are the targets of miR-199a. To further corroborate this, we transfected Cy3-labeled miR-199a mimics into SMMC-7721 cells (which show a low level of endogenous *mir-199a* expression; Appendix Fig S4A), and found that both HK2 and PKM2 staining signals were greatly reduced in miR-199a-transfected cells compared with control cells (Fig 3C). Western blot further confirmed that HK2 and PKM2 protein levels were dramatically reduced in both Hep3B and SMMC-7721 cells transfected with miR-199a mimics, while qRT–PCR analyses showed that their mRNA levels were moderately reduced (Fig 3D and Appendix Fig S4B). In contrast, inhibition of miR-199a by anti-miR-199a in Hep3B cells (which have higher endogenous *mir-199a* expression; Appendix Fig S4A) led to enhanced *Hk2* and *Pkm2* expression (Fig 3D, bottom). These results together reveal *Hk2* and *Pkm2* as authentic and direct targets of miR-199a.

miR-199a represses *Hk2* and *Pkm2* in hypoxic HCC cells via two distinct mechanisms

We further examined the effect of miR-199a on *Hk2* and *Pkm2* expression in hypoxic HCC cells. Hypoxia treatment strongly increased both protein and mRNA levels of *Hk2* and *Pkm2* in Hep3B cells (Fig 3E, left, lane 2), whereas transfection of miR-199a mimics completely overrode this effect of hypoxia on HK2 and PKM2 protein expression (lane 4). Intriguingly, we observed that miR-199a overexpression also robustly reduced *Hk2* and *Pkm2* mRNAs in hypoxic HCC cells (Fig 3E, right, blue column), suggesting that miR-199a may employ an additional mechanism to regulate *Hk2* and *Pkm2* in hypoxic cells. Of note, *HIF-1α*, which encodes the O_2-regulated subunit of HIF-1, is a known target of miR-199a (Yeligar *et al*, 2009), implying that miR-199a may inhibit the transcription of *Hk2* and *Pkm2* in hypoxic HCC cells through targeting *HIF-1α*. Indeed, under hypoxic condition, the protein level of HIF-1α was significantly decreased along with reduction of HK2 and PKM2 proteins in miR-199a mimic-transfected Hep3B cells (Fig 3E, right, lane 4), supporting that *HIF-1α* is targeted by miR-199a in HCC cells. As expected, co-transfection of a miR-199a-resistant form of *HIF-1α* (its 3′ UTR is missing) completely restored *Hk2* and *Pkm2* mRNA levels in cells overexpressing miR-199a (Fig 3E, right). However, ectopic HIF-1α expression had little effect on HK2 and PKM2 protein expression in these cells (Fig 3E, left, lane 5), further supporting that miR-199a also controls HK2 and PKM2 production at the posttranscriptional level. These results thus reveal that miR-199a employs two distinct mechanisms to repress *Hk2* and *Pkm2* expression in hypoxic HCC cells. Additionally, depleting HuR protein in these cells effectively attenuated the stimulatory effect of hypoxia on HK2 and PKM2 protein expression (Appendix Fig S4C, lane 4), despite little association between HuR and their mRNAs (Appendix Fig S4D). This is consistent with our above finding that HuR is required for inhibiting *mir-199a* maturation (Fig 2), further supporting that miR-199a is critical to repressing *Hk2* and *Pkm2*. Taken together, these results support the idea that *mir-199a* down-regulation is required for hypoxia-activated HK2 and PKM2 expression in HCC cells.

The miR-199a:*Hk2*/*Pkm2* axis is functionally important for regulating glycolysis in HCC cells

We next examined whether this newly discovered miR-199a:*Hk2*/*Pkm2* axis is involved in regulating glucose metabolism in HCC cells. Transfection of miR-199a mimics in either Hep3B or SMMC-7721 cells significantly reduced the rates of glucose consumption and lactate and ATP production (Fig 4A and Appendix Fig S5A). Correspondingly, microPET/CT imaging assays showed that [^{18}F]FDG uptake (as normalized to tumor mass) was significantly lower in engrafted miR-199a-overexpressing Hep3B or SMMC-7721 tumors than in control RNA-transfected tumors (Fig 4C and Appendix Fig S5B). We then performed the reciprocal experiment by using anti-miR-199a to inhibit miR-199a in Hep3B cells and found that transfection of anti-miR-199a dramatically accelerated glycolysis in cultured cells and enhanced [^{18}F]FDG uptake in xenograft tumors (Fig 4B and D). These results together indicate that miR-199a is a repressor for glucose metabolism in HCC cells.

We next examined whether miR-199a exerts its inhibitory effects on glucose metabolism by targeting *Hk2* and *Pkm2*. In line with the pivotal roles of HK2 and PKM2 in cancer cell metabolism (Mathupala *et al*, 2009; Luo & Semenza, 2012), either *Hk2* or *Pkm2* knockdown by siRNA robustly decreased glucose metabolism in cultured SMMC-7721 cells (which have higher endogenous HK2 and PKM2 expression; Appendix Fig S4A) and significantly decreased glucose metabolism in cultured cells and [^{18}F]FDG uptake in xenograft tumors (Appendix Fig S6). These results indicate that RNAi-mediated silencing of *Hk2* or *Pkm2* recapitulates the inhibitory effect of miR-199a on glycolysis in HCC cells. To verify the functional role of the miR-199a:*Hk2*/*Pkm2* axis in regulating glucose metabolism in

Figure 4. miR-199a inhibits glucose metabolism in HCC cells and tumors by targeting *Hk2* and *Pkm2*.

A, B The effect of miR-199a on glucose metabolism in cultured Hep3B cells. The rates of [^{18}F]FDG uptake (upper left), lactate production (upper right), and ATP production (lower left) in miR-199a mimic- (A) or anti-miR-199a-transfected Hep3B cells (B) were determined 24 h post-transfection. Lower right, Western blot of HK2 and PKM2 proteins in transfected cells.

C, D The effect of miR-199a on [^{18}F]FDG uptake in xenograft Hep3B tumors. MicroPET/CT imaging of mice for determining [^{18}F]FDG uptake in miR-199a mimic- (C) or anti-miR-199a-transfected Hep3B tumors (D) at 2–3 weeks after tumor cell inoculation. Left, representative microPET/CT images; arrowheads indicate xenograft HCC tumors; right, quantification of [^{18}F]FDG uptake in tumors (in % ID/g tumor) (n = 4–5 mice per group).

E, F Restoration of *Hk2* or *Pkm2* expression overrode the inhibitory effects of miR-199a on glucose metabolism in cultured Hep3B cells (E) and [^{18}F]FDG uptake in Hep3B tumors (F).

Data information: The average values ± SD of three separate experiments are plotted. Statistics: Student's t-test; *$P < 0.05$, **$P < 0.01$.
Source data are available online for this figure.

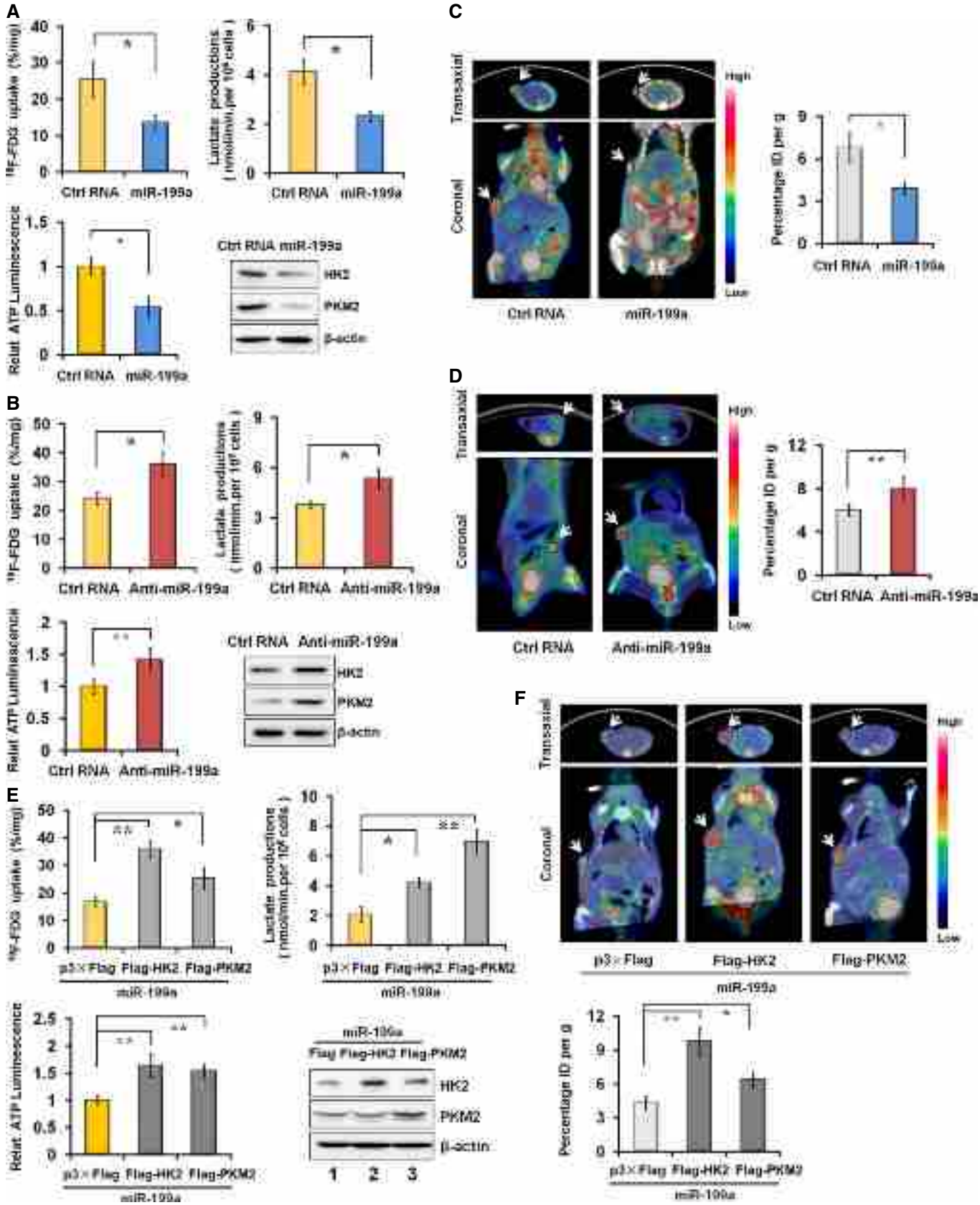
A
B
C
D
E
F
Ctrl RNA
miR-199a
Anti-miR-199a
HK2
PKM2
β-actin
Transaxial
Coronal
High
Low
p3×Flag
Flag-HK2
Flag-PKM2

Figure 4.

HCC cells, we constructed miR-199a-resistant expression vectors (p3xFlag-HK2 and p3xFlag-PKM2; without their 3′ UTRs) for ectopic expression of HK2 or PKM2 proteins. Co-transfection of these vectors largely rescued the impact of miR-199a on glycolysis in cultured Hep3B or SMMC-7721 cells as well as [^{18}F]FDG uptake in xenograft tumors (Fig 4E and F, and Appendix Fig S7), supporting the idea that targeting *Hk2* and *Pkm2* is an important mechanism of miR-199a-mediated suppression of glycolysis in HCC cells. Collectively, these results indicate that the miR-199a:*Hk2/Pkm2* axis is of functional importance in regulating glucose metabolism in HCC cells.

The miR-199a:*Hk2/Pkm2* axis plays a functional role in controlling tumorigenesis in HCC cells

In addition to their established roles in cell metabolism, both HK2 and PKM2 are also oncogenic proteins that are important for cancer progression (Mathupala *et al*, 2009; Luo & Semenza, 2012). We thus asked whether the miR-199a:*Hk2/Pkm2* axis plays a role in regulating tumorigenesis of HCC cells. As expected, transfection of miR-199a mimics in Hep3B or SMMC-7721 cells strongly reduced cell proliferation, cell survival, anchorage-independent growth, and transwell cell migration as well as the rate of xenografted tumor growth in nude mice (Appendix Fig S8A and B). Conversely, inhibition of miR-199a function by anti-miR-199a in Hep3B cells markedly increased cell proliferation and migration in cultured cells and tumor growth in nude mice (Appendix Fig S8C), indicating that miR-199a negatively regulates HCC tumorigenesis. We next examined whether miR-199a exerts its tumor-suppressive effects in HCC cells by targeting *Hk2* and *Pkm2*. RNAi knockdown of *Hk2* or *Pkm2* reproduced the phenotype observed with miR-199a overexpression in SMMC-7721 cells (Appendix Fig S9). Importantly, co-transfection of miR-199a-resistant *Hk2* or *Pkm2* in miR-199a-transfected Hep3B or SMMC-7721 cells strongly overrode the effects of miR-199a on HCC tumorigenesis *in vitro* and *in vivo* (Fig 5 and Appendix Fig S10). Collectively, these results indicate that the miR-199a:*Hk2/Pkm2* axis plays important roles in regulating tumorigenesis of HCC cells.

The hypoxia-miR-199a-*Hk2/Pkm2* regulatory axis functions in HCC tumors

We next asked whether the miR-199a-HK2/PKM2 axis is indeed regulated by hypoxia in HCC tumors. To address this, we first examined intratumoral hypoxia in xenografted SMMC-7721 tumors at 14, 21, and 28 days after tumor cell inoculation. Immunohistochemical assays of tumor sections for pimonidazole hydroxychloride (Hypoxyprobe-1) showed that intratumoral hypoxia increased over time (Appendix Fig S11A). Interestingly, as intratumoral hypoxia increased, miR-199a level decreased as revealed by FISH (Appendix

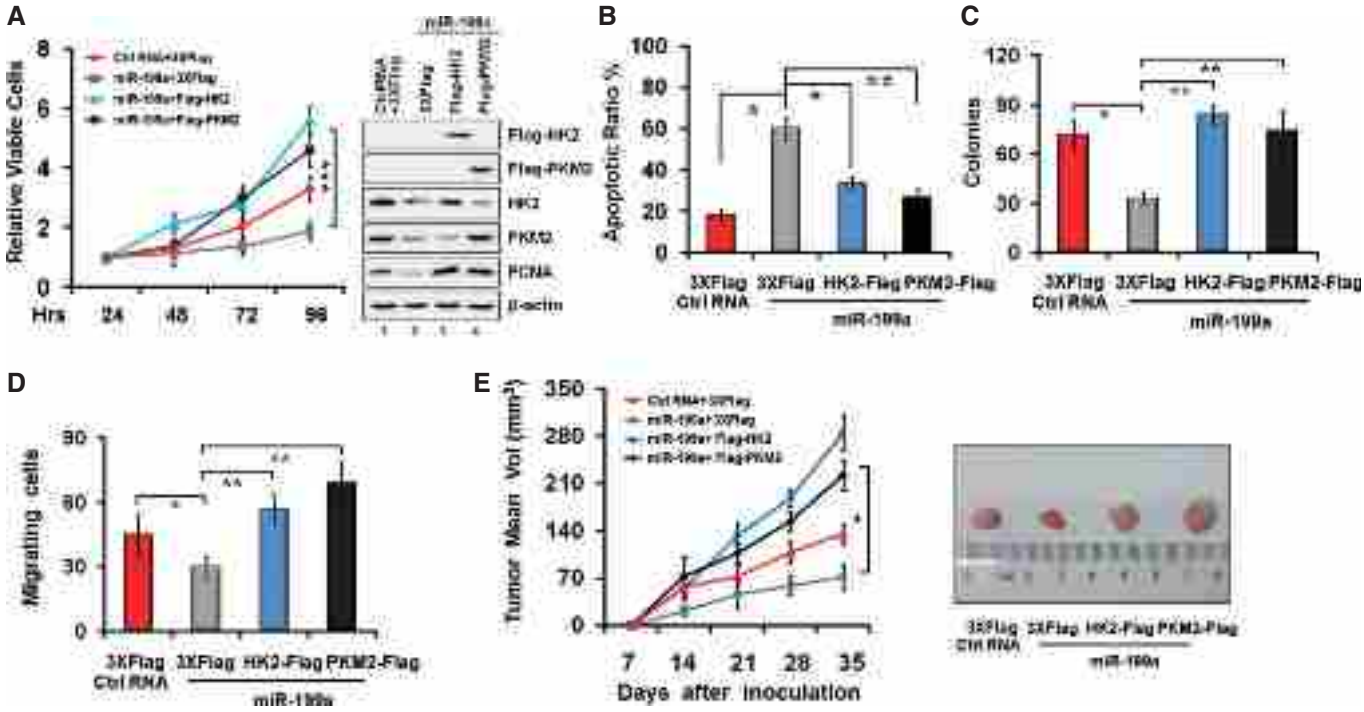

Figure 5. The miR-199a-*Hk2/Pkm2* axis is of functional importance in regulating tumorigenesis in HCC cells.

A–E Ectopic expression of Flag-HK2 or Flag-PKM2 in Hep3B cells transfected with miR-199a mimics significantly attenuated the effects of miR-199a on cell proliferation (A), cell apoptosis (B), soft agar colony formation (C), transwell cell migration (D), and xenograft tumor growth in nude mice (E). (A) Left, MTT assays; right, Western blot analyses of HK2, PKM2, and PCNA proteins. (E) Left, the time course of tumor growth (n = 4–5 mice per group); right, representative xenograft tumors at 35 days after inoculation. The average values ± SD of three separate experiments are plotted. Statistics: Student's t-test; *$P < 0.05$, **$P < 0.01$, ***$P < 0.001$.

Source data are available online for this figure.

Fig S11B) and there was a concomitant increase in HK2 and PKM2 proteins as shown by immunostaining (Appendix Fig S11C), supporting that the hypoxia-miR-199a-HK2/PKM2 regulatory axis is functional *in vivo*.

Systemic agomiR-199a delivery effectively inhibits tumor growth and [^{18}F]FDG uptake in HCC tumor-bearing mice

We next performed a treatment study, asking whether restoration of miR-199a expression has a therapeutic effect on HCC tumors. To this end, we injected a cholesterol-modified and Cy3-labeled miR-199a oligo (agomiR-199a) formulated with a lipid-based delivery reagent into the tail veins of NOD-SCID mice 2 weeks after subcutaneous SMMC-7721 cell implantation, with one injection every 3 days for seven cycles (Fig 6A; $n = 5–6$). Two negative control (NC) groups received Cy3-labeled agomiR-NC or PBS treatments.

Systemic delivery of agomiR-199a effectively inhibited tumor growth compared with agomiR-NC or PBS controls (Fig 6B). Moreover, concurrent microPET/CT imaging showed that [^{18}F]FDG uptake in HCC tumors from the agomiR-199a-treated group was dramatically reduced at day 21, but this reduction was not observed in the agomiR-NC- or PBS-treated groups (Fig 6C and D). Notably, [^{18}F]FDG microPET/CT imaging further confirmed that the growth of agomiR-199a-treated tumors was greatly attenuated compared with controls (Fig 6C). At day 24, we euthanized all mice and harvested xenografted tumors for further analyses. Again, we found that agomiR-199a strongly reduced tumor burden (by > 50%) compared with agomiR-NC or PBS controls (Fig 6E). qRT–PCR showed that the miR-199a levels in agomiR-NC- or PBS-treated SMMC-7721 tumors were significantly reduced relative to that in cultured cells, but agomiR-199a delivery effectively augmented miR-199a expression in HCC tumors (Fig 6F). Consistently, Cy3 signals were readily detectable in tumors from agomiR-treated mice but not in PBS-treated controls (Fig 6G, left panels), indicating successful uptake of Cy3-labeled oligos into tumors. Immunohistochemical staining showed that HK2 and PKM2 protein levels were significantly reduced in HCC tumors from agomiR-199a-treated mice compared with controls (Fig 6G, middle panels). We further found that the cell proliferation marker PCNA declined in tumors from agomiR-199a-treated mice compared with those in controls (right panels), supporting the idea that miR-199a inhibits cell proliferation in HCC tumors. These results together indicate that miR-199a has therapeutic efficacy against HCC tumors.

We also assessed the potential toxicity of agomiR treatment on tested mice. We found that all mice remained healthy and similarly gained weight during the course of the therapeutic experiments (Appendix Fig S12A). ELISA of cleaved caspase-3 activity showed that agomiR administration did not have obvious toxic effects on the liver or other organs (Appendix Fig S12B), although immunostaining of liver sections for F4/80 showed a moderate increase in Kupffer cell macrophages in agomiR-treated mice (Appendix Fig S12C). Clinical blood chemistry further confirmed that agomiR administration does not affect the physiology of tested mice (Appendix Fig S12D). Taken together, these results indicate that agomiR-199a treatment at the dosage and frequency used in our study showed little toxic effect on the overall health of tested animals.

The expression of *HuR*, *mir-199a*, HK2, and PKM2 is correlated in human HCC specimens

To test whether our above findings in HCC cells are clinically relevant, we examined the miR-199a levels as well as the levels of *HuR*, *Hk2*, and *Pkm2* mRNAs in 65 human HCC primary tumor and paired adjacent normal tissue specimens. qRT–PCR showed that *mir-199a* was significantly down-regulated in HCC tumors compared to normal tissues (Fig 7A), while expression of *HuR*, *Hk2*, and *Pkm2* was significantly up-regulated (Fig 7B and C; Appendix Fig S13A). Importantly, we observed significantly lower miR-199a expression and significantly greater *Hk2* and *Pkm2* expression in HCC tumors with higher *HuR* expression (Appendix Fig S13B). We found a significant inverse correlation between miR-199a and *Hk2* mRNA levels (Pearson's $R = -0.564$, $P < 0.05$; Fig 7D), or *Pkm2* mRNA levels in tumor specimens ($R = -0.452$, $P < 0.05$; Fig 7E). We further found that HCC tumors with higher miR-199a levels showed weaker HK2 and PKM2 immunohistochemical staining (Fig 7F; left), whereas tumors with less miR-199a expression showed stronger HK2 and PKM2 staining (right). Collectively, these results strongly suggest that the HuR-miR-199a:*Hk2*/*Pkm2* regulatory axis that we have discovered is clinically relevant in HCC.

Discussion

The causative roles of intratumoral hypoxia in reprogramming cancer cell metabolism have been well established, with HIF-1-mediated transcriptional regulation being important as it controls several genes crucial to deregulated metabolism in cancers, that is, the Warburg effect (Semenza, 2010). However, the role of miRNAs in hypoxia-altered cancer cell metabolism remains poorly understood. We have shown that the miR-155/miR-143 cascade controls glycolysis by regulating *Hk2* expression in breast cancer cells (Jiang *et al*, 2012), demonstrating that miRNA regulation is of functional importance in regulating glucose metabolism in cancer cells. Of note, a recent study indicates that breast cancer cell-secreted miR-122 suppresses glucose uptake by niche cells and facilitates metastasis by targeting pyruvate kinase (Fong *et al*, 2015). In the present study, we found that hypoxia down-regulates miR-199a and that down-regulation of *mir-199a* is crucial for the glycolysis-promoting effect of hypoxia in HCC cells. Mechanistically, hypoxia promotes binding of the RNA-binding protein HuR to pri-miR-199a and consequently blocks miR-199a maturation. Recent studies have shown that miR-199a plays a tumor-suppressive role in cancers by negatively regulating different targets (Yeligar *et al*, 2009; Cheng *et al*, 2012; Tsukigi *et al*, 2012; Hu *et al*, 2014). Nevertheless, its role in cancer metabolism has not been reported. Our results here showed that miR-199a robustly suppresses glycolysis in HCC cells and it does so through repressing *Hk2* and *Pkm2*, two key glycolytic genes in cancers (Mathupala *et al*, 2009; Luo & Semenza, 2012). Of note, miR-155, a miRNA that we have previously shown to promote glucose metabolism by up-regulating *Hk2* in breast cancer cells (Jiang *et al*, 2012), is potently up-regulated in hypoxic HCC cells. This implicates that miR-155 up-regulation in hypoxic HCC cells should have a complimentary role to miR-199a down-regulation in

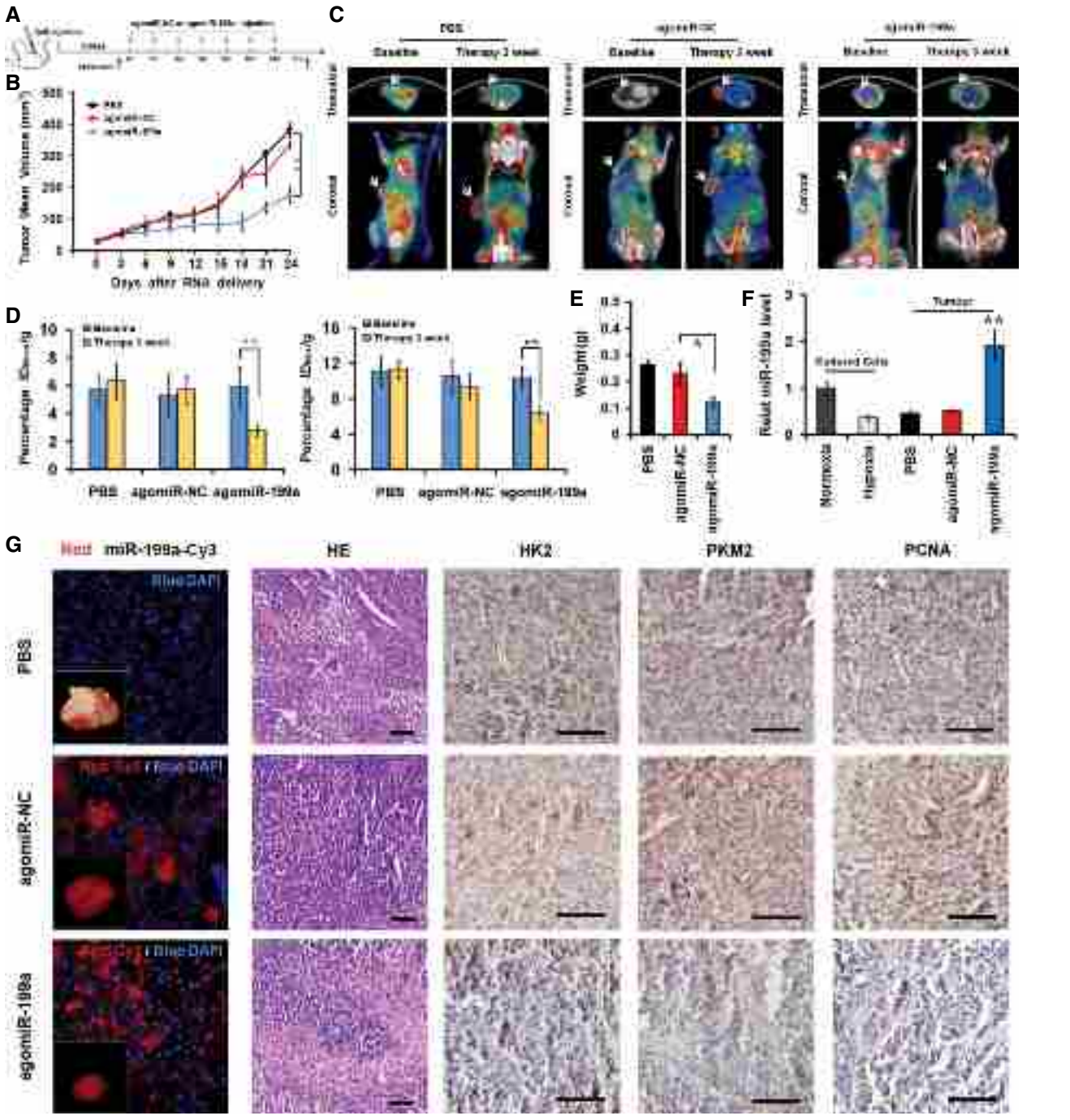

Figure 6. Systemic delivery of agomiR-199a inhibits tumor growth and [^{18}F]FDG uptake in HCC tumors in nude mice.

A Schematic diagram illustrating the experimental design. Intravenous delivery of agomiR started at 2 weeks after subcutaneous implantation of SMMC-7721 cells in NOD-SCID mice (day 0). The mice received treatments with PBS or seven doses of 50 mg/kg agomiR every 3 days through day 18.

B The time course of SMMC-7721 tumor growth in mice treated with agomiR-199a or agomiR-NC or PBS (negative controls).

C, D MicroPET/CT imaging of mice to determine [^{18}F]FDG uptake in SMMC-7721 tumors in mice treated with PBS, agomiR-NC, or agomiR-199a at baseline (day 0) or treatment end (day 21). Representative [^{18}F]FDG microPET images are shown with arrowheads indicating xenografted HCC tumors (C). Quantification of [^{18}F]FDG uptake in tumors is shown as $\%ID_{mean}$/g and $\%ID_{max}$/g tumor (D).

E Weight of SMMC-7721 tumors in each group at day 24.

F Comparison of miR-199a levels as determined by qRT–PCR between SMMC-7721 cells cultured in normoxic or hypoxic conditions and SMMC-7721 tumors from three groups.

G Cy3 imaging (red), hematoxylin and eosin (HE), or HK2, PKM2, or PCNA immunohistochemical staining (brown) of SMMC-7721 tumor sections from three groups. Left panels, inset is the representative tumor at day 24, and magnification for tumor sections is 20×. Scale bars for right panels, 100 μm.

Data information: All data are mean ± SD of three separate experiments. Statistics: Student's *t*-test; $^*P < 0.05$, $^{**}P < 0.01$; $n = 5$–6 in each group.

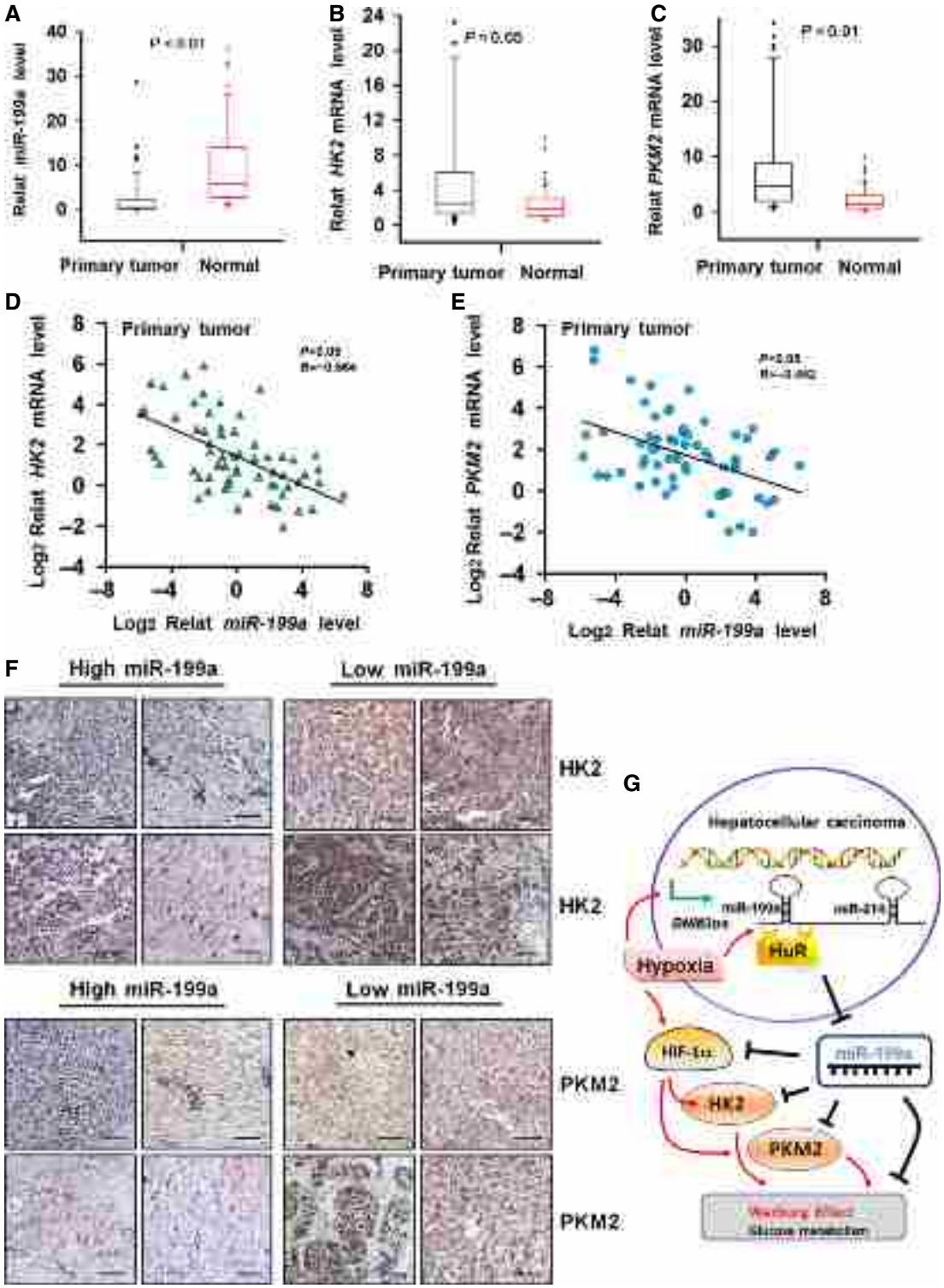

Figure 7. Comparison of miR-199a, *Hk2*, and *Pkm2* expression in human HCC specimens.

A–C Boxplots of expression of miR-199a (A), *Hk2* (B), and *Pkm2* (C) in 65 human HCC and paired normal adjacent tissues. The expression levels of miR-199a, *Hk2* and *Pkm2* were determined by qRT-PCR. The boxes represent the median (middle line) between the 25th (Q1) and 75th (Q3) percentiles. The whiskers are the upper and lower adjacent values. Significant differences in expression between tumors and control tissues were assessed using Student's *t*-test.

D, E Pearson's correlation analyses of miR-199a and *Hk2* (D) or *Pkm2* mRNA levels (E) in 65 human HCC specimens. Statistics: Pearson's correlation analyses.

F Representative images of HK2 (top) and PKM2 (bottom) immunohistochemical staining (brown) of human HCC sections with high (left) or low miR-199a expression (right), with sections counterstained by Mayer hematoxylin (blue). Scale bar, 100 μm.

G Model of miR-199a as a key regulatory node linking hypoxia to deregulated glucose metabolism in HCC.

regulating glucose metabolism in HCC cells. Collectively, our findings indicate miR-199a is a master regulator in hypoxia-deregulated cancer glucose metabolism (Fig 7G), providing substantial new mechanistic insights into hypoxia-induced deregulated glucose metabolism in cancer cells.

Tumor cell metabolism is clearly linked with cancer outcomes, and targeting metabolic enzymes has been extensively studied for cancer therapy (Kroemer & Pouyssegur, 2008; Vander Heiden, 2011). But such an antineoplastic strategy has also raised concerns given that targeting metabolic enzymes would have unacceptable effects on normal cells (Vander Heiden, 2011). In the present study, we showed that miR-199a, by suppressing two key glycolytic genes, *Hk2* and *Pkm2*, inhibits both glucose metabolism and tumorigenesis in HCC cells. Most recently, an independent article reported that *Hk2* is a target of miR-199a in HCC cells (Guo *et al*, 2015), confirming that miR-199a plays a critical role in regulating glycolysis in liver cancer. Importantly, our data showed that systemic delivery of cholesterol-modified agomiR-199a to mice effectively inhibits the growth of xenografted HCC tumors as well as [^{18}F]FDG uptake in these tumors, indicating a strong rationale for developing miR-199a as a novel metabolism-targeting therapeutic agent against HCC. Moreover, we note a recent study showing that miR-199a inhibits tumor angiogenesis (Raimondi *et al*, 2014), further supporting this miRNA as a strong target candidate for anticancer therapies.

In addition, miR-199a and miR-214 are clustered in DNM3os, a lncRNA (Lee *et al*, 2009), but their expression pattern and function in human cancers are quite the opposite. Namely, miR-199a is usually down-regulated in tumors and plays a tumor suppressor role in cancer cells (Yeligar *et al*, 2009; Cheng *et al*, 2012; Tsukigi *et al*, 2012; Hu *et al*, 2014), whereas miR-214 is often up-regulated in cancers and acts as an oncomiR, functioning in tumor progression and metastasis (Yang *et al*, 2008; Ueda *et al*, 2010; Penna *et al*, 2011). However, little is known how miR-199a and miR-214 in cancer cells are differentially expressed from same miRNA cluster. Intriguingly, we found that hypoxia selectively blocks pri-miR-199a processing but barely affects the maturation of miR-214 in human HCC cells, suggesting that how hypoxic stress governs the pathway by which the two miRNAs are processed is distinctly regulated. Interestingly, the RNA-binding protein HuR, which has been reported to link mRNA stability to the hypoxic response (Galban *et al*, 2008; Hinman & Lou, 2008; Masuda *et al*, 2009), was characterized as a key mediator of the inhibitory effect of hypoxia on pri-miR-199a processing. Our findings thus document a novel function of HuR —namely regulation of noncoding RNAs during hypoxia in human cancer cells. Of note, a recent study showed that during hemodynamic stress, cardiac hypoxia increases both miR-199a and miR-214 levels in hearts from mice along with up-regulating *DNM3os* (el Azzouzi *et al*, 2013), which appears to be opposite to our observation in human HCC cells. Intriguingly, we found no potential HuR-binding sites in the mouse pri-miR-199a transcript, and that hypoxia barely modulated *mir-199a* expression in the mouse HCC cell line Hepa1-6 (data not shown). This suggests that the HuR-mediated suppression of pri-miR-199 processing is likely a human cell-specific event.

In summary, our study reveals HuR-miR-199a:*Hk2/Pkm2* to be a novel pathway linking hypoxia to deregulated glucose metabolism in HCC cells and shows the therapeutic effect of systemically delivered agomiR-199a on HCC. Given that targeting tumor metabolism is extensively studied as therapeutic approach for cancer (Vander Heiden, 2011), miRNA molecules like miR-199a could serve as novel candidate targets in addition to metabolic enzymes for such antineoplastic strategies. Additionally, epidemiologic data have recognized HBV/HCV infection, alcoholic liver disease, and non-alcoholic steatohepatitis as major risk factors for HCC (El-Serag, 2011). It will be interesting in future studies to determine whether this newly discovered HuR-miR-199a:*Hk2/Pkm2* axis is distinct in HCC etiology.

Materials and Methods

Cell culture and transfection

All cell lines were cultured at 37°C, 5% CO_2 in Dulbecco's modified Eagle's medium (DMEM) supplemented with 10% fetal bovine serum and 1% penicillin/streptomycin. The Hep3B and embryonic kidney cell line HEK293T cells were obtained from the American Type Culture Collection (ATCC), and SMMC-7721 cells were from Cell Resource Center. For hypoxia stimulation, cells were transferred to a hypoxia chamber with 1% oxygen. Transfection was performed using Lipofectamine 2000 (Invitrogen) according to the manufacturer's instructions. For transfection of the RNA oligonucleotides, 50 nmol/l of miRNA mimics and 100 nmol/l of antisense oligonucleotides were used except where indicated otherwise. For plasmids, 4 μg DNA was used in a 6-well plate. In the rescue experiments, cells were co-transfected with 25 nmol/l miRNA mimics and 2 μg plasmid DNA in a 6-well plate. G418 (200 μg/ml) was added 24 h after transfection.

Plasmid constructs, RNA oligonucleotide, and antibodies

Human *Hk2*, *Pkm2,* and *HIF-1α* cDNAs without their 3′ UTRs were cloned into the p3xFlag-CMV-14 expression vector (Sigma) to construct p3xFlag-HK2, p3xFlag-PKM2, and p3xFlag-HIF-1α vectors, respectively. The pri-miR-199a-2 sequences were cloned into pLenti-EF1a-EGFP for generating the pri-miR-199a-2 expression vector. Two predicted HuR-binding sites were deleted in the Mut-1 and Mut-2 pri-miR-199a-2 vector (Fig 2G). For reporters pRL-TK-HK2-3′UTR and pRL-TK-PKM2-3′UTR, human ~2.4-kb *Hk2* and ~620-bp *Pkm2* 3′ UTRs were cloned downstream of the *Renilla* luciferase coding sequences in pRL-TK (Promega), and eight nucleotides in the 3′ UTR corresponding to 5′ UTR of miR-199a were deleted in the Mut constructs (Fig 3A). All the constructs were confirmed by DNA sequencing. The agomiR-199a, miR-199a mimics, anti-miR-199a, small interfering RNAs (siRNAs) targeting *Hk2*, *Pkm2*, *HuR*, *NF90*, *MSI2*, *Lin28B* or *YAP*, and their respective negative control RNAs were purchased from RiboBio (Guangzhou, China). The siRNA sequences are provided in Appendix Table S1. Antibodies for Lin28B, YAP, HK2, PKM2, and caspase-3 were from Cell Signaling. The antibody for HuR was from Invitrogen, and antibody for PCNA was from Abcam. Antibodies for F4/80, NF90, and MSI2 were from Proteintech. Antibodies for Flag, Dicer, DGCR8, and β-actin, as well as Cy3- or Alexa Fluor-488-conjugated donkey anti-rabbit IgG, were from Sigma.

Biochemical and cell biology assays

Western blot, immunofluorescence, immunohistochemistry, histology, Northern blot, FISH, and luciferase reporter assays were carried out as we described recently (Jiang *et al*, 2012; Zhao *et al*, 2013; Wang *et al*, 2014). The band intensities in Western and Northern blots were quantified with an LAS4000 Image Analyzer. Cy3- or Alexa Fluor-488-conjugated donkey anti-rabbit IgG (Sigma) was used as secondary antibody to visualize HK2 and PKM2 in immunofluorescence assays, with nuclei counterstained by DAPI (Vector Laboratories). For immunohistological stains, tumor sections were first incubated with a primary antibody against the tested protein and then incubated with biotinylated secondary antibody after washing with PBS, followed by a further incubation with the streptavidin–horseradish peroxidase complex. After that, the sections were counterstained with hematoxylin. For histological analysis, paraffin-embedded tumor sections were stained with hematoxylin and eosin. For Northern blot, [^{32}P]-labeled probes were used. For FISH, we used Cy3-labeled RNA probes complementary to miR-199a or the upstream sequences of hairpin pre-miRNA to detect mature miR-199a or pri-miR-199a. The oligonucleotide probe sequences are provided in Appendix Table S1.

RNA isolation, quantitative reverse transcription PCR (qRT–PCR), and RNA immunoprecipitation (RIP) assays

The assays were performed as we described recently (Zhao *et al*, 2013). In brief, the levels of pri-miRNAs were quantified using the TaqMan® Pri-miRNA assay kit (Stem-loop Accession #MI0000281 for pri-miR-199a-2,Stem-loop Accession #MI0000242 for pri-miR-199a-1,Stem-loop Accession #MI0000290 for pri-miR-214; Applied Biosystems by Life Technology). The levels of mature miRNAs were quantified using TaqMan® MicroRNA Assay kits (Applied Biosystems by Life Technology). The primer sequences for qRT–PCR are provided in Appendix Table S1. The qRT–PCR results were analyzed and shown as relative miRNA or mRNA levels of the CT (cycle threshold) values, which were then converted as fold change. For RIP assays, cells were homogenized in lysis buffer [100 mM KCl, 5 mM $MgCl_2$, 10 mM HEPES, 0.5% NP-40 containing 10 U/ml RNase inhibitor (Takara) and a protease inhibitor cocktail (Roche)]. Cell extracts were incubated with anti-HuR or IgG-coupled protein A/G beads for 4–6 h. After stringently washing the beads with washing buffer (50 mM Tris–HCl [pH 7.4], 150 mM NaCl, 1 mM $MgCl_2$, and 0.05% NP-40, protease inhibitor cocktail, and RNase inhibitor), total RNAs were extracted with TRIzol and subjected to RT–PCR assays.

Cell proliferation, apoptosis, soft agar colony formation, transwell migration, and xenograft assays

These assays were performed as we described recently (Wang *et al*, 2014). In brief, HCC cells were transfected with RNA oligonucleotide and/or plasmid DNA. At 24 h post-transfection, equal numbers of viable cells were seeded in 96-well plates for MTT cell proliferation or apoptosis assays, or mixed with 1.5 ml 1640 RPMI medium with 0.4% soft agar for soft agar colony formation assay, or plated in the upper transwell chamber in 300 μl serum-free 1640 RPMI medium for cell migration assay, or injected subcutaneously into male BALB/c athymic nude mice (n = 6) at 6–8 weeks of age for tumor engraftment. Tumors were examined every 5 days for a total of 35 days. Tumor growth rates were analyzed by measuring tumor length (L) and width (W) and calculating the volume with the formula $LW^2/2$.

Measurement of glucose consumption and lactate and ATP production

Glucose consumption and lactate production were analyzed with a glucose assay kit (Sigma) and lactate assay kit (Biovision) as we previously described (Jiang *et al*, 2012). For [^{18}F]-FDG uptake experiments, HCC cells were washed with glucose-free medium 24 h post-transfection and then cultured in glucose-free RPMI medium containing 1 μCi/ml [^{18}F]FDG. After 60-min incubation, cells were lysed in RIPA buffer after stringent washes with ice-cold PBS, and then, [^{18}F] incorporation was counted using an automated gamma counter. Protein concentration of each sample was determined using a Bradford protein assay kit (Promega) with BSA as the standard according to the manufacturer's recommendations. The relative [^{18}F]FDG uptake was normalized according to the respective cell lysate protein concentration. The cellular ATP level in HCC cells was determined at 24 h post-transfection with a CellTiter-Glo 2.0 Assay kit (Promega) and luminometer (Promega) according to the manufacturer's protocols. The relative ATP levels (measured as luminescence) were normalized to the respective cell lysate protein concentration.

Intratumoral hypoxia assay

Pimonidazole hydroxychloride with immunochemical reagents (Hypoxyprobe-1) has been used as a hypoxia marker to detect hypoxic cells in various tissues *in vivo*, due to its reductive metabolism being sensitive to oxygen tension (Arteel *et al*, 1998). The tumor-harboring mice were administrated intravenously by tail vein injection 10 mg/20 g body wt of Hypoxyprobe-1 (Natural Pharmacia International) 1 h before animals were sacrificed. Then, all engrafted HCC tumors were immediately excised for hypoxia assay. In brief, tumor sections were stained with rabbit anti-Hypoxyprobe antibody (Natural Pharmacia International), followed by staining with Alexa Fluor 647-labeled anti-rabbit IgG antibody (Invitrogen). Nuclei were counterstained with DAPI (Vector Laboratories).

MicroPET/CT imaging of mice

MicroPET/CT imaging of mice was performed as we described previously (Jiang *et al*, 2012). In brief, tumor-bearing mice were placed on a dedicated small animal microPET/CT scanner (Siemens Inveon MM STD MicroPET/CT 3074; Siemens) 40 min after injection of 100–200 μCi [^{18}F]FDG via tail vein. Mice were first subjected to a 15-min microCT scan and then to a 10-min microPET scan. microPET and microCT images were analyzed with Inveon software (Siemens). Regions of interest (ROIs) were manually drawn by qualitative assessment covering the entire tumor. Tumor volumes were generated by summing voxels within the tomographic planes. The ROI counts were converted to the % ID/g tumor using filtered back projection as previously described (Tseng *et al*, 2008).

Therapeutic experiments

For *in vivo* treatment assays, we established SMMC-7721 subcutaneous tumors in ~6-week-old NOD-SCID mice (n = 5–6) and allowed tumors to grow for approximately 2 weeks to reach a volume of 30–40 mm^3. When tumors had formed, mice were administrated intravenously by tail vein injection 35 mg/20 g Cy3-labeled agomiR-199a or scrambled negative control RNA (miR-NC) respectively on days 0, 3, 6, 9, 12, 15, and 18 (Fig 7A). The chemically modified agomiRs were formulated with a lipid-based delivery reagent (Wiggins *et al*, 2010). The animals were imaged on days 0 and 21 using [^{18}F]FDG microPET/CT. Blood samples were collected for blood chemistry analyses on day 24 before animals were sacrificed. Finally, all HCC tumors and major organs were excised for further analyses. The cholesterol-modified and Cy3-labeled agomiR-199a and miR-NC were commercially synthesized by RiboBio (Guangzhou, China).

Statistical analyses

All results were presented as the mean ± SD. A Student's t-test was performed to compare the differences between treated groups relative to their paired controls. One-way ANOVA was used to analyze tumor growth data. P-values are indicated in the text or figures above the two groups compared with a value < 0.05 (denoted by asterisks) considered significant (***$P < 0.001$, **$P < 0.01$). Pearson's correlation analyses were used to calculate the regression and correlation between two groups.

Study approval

HCC specimens and paired normal adjacent tissues were collected during surgery from Eastern Hepatobiliary Surgery Hospital (Shanghai, China) with written informed consent from patients. Samples were immediately snap-frozen and stored at −80°C. The specimen collection was approved by the Medical Ethical Committee of the hospital. All animal experiments were performed under protocols approved by the Shanghai Institute of Biochemistry and Cell Biology and University of Louisville and in accordance with the Guide for the Care and Use of Laboratory Animals (NIH publication nos. 80-23, revised 1996).

Expanded view for this article is available online:
http://emboj.embopress.org

Acknowledgements
This work was supported by grants from the Ministry of Science and Technology of China (2012CB910803, 2014CB943103, 2011CB811303, and 2014CB964802), National Natural Science Foundation of China (31170754, 31325008, 91419307, 31300656, and 91219306), Science and Technology Commission of Shanghai Municipality (13ZR1464300), and Chinese Academy of Sciences (KJZD-EW-L01-2 and 2013KIP202). YL is supported by CA138688 (NIH). The authors are grateful to Dr. Cassandra Talerico for her critical reading of this manuscript.

Author contributions
LFZ and MFL planned the project; LFZ, YL, DL, and MFL designed the experiments; LFZ, JTL, MHL, CG, SZ, BL, and SL performed the experiments; LFZ, BL, SL, and MFL analyzed the data; LFZ, YL, DL, and MFL wrote the manuscript; all authors discussed the results and commented on the manuscript; and MFL supervised the study.

Conflict of interest
The authors declare that they have no conflict of interest.

References

Airley RE, Mobasheri A (2007) Hypoxic regulation of glucose transport, anaerobic metabolism and angiogenesis in cancer: novel pathways and targets for anticancer therapeutics. *Chemotherapy* 53: 233 – 256

Arteel GE, Thurman RG, Raleigh JA (1998) Reductive metabolism of the hypoxia marker pimonidazole is regulated by oxygen tension independent of the pyridine nucleotide redox state. *Eur J Biochem* 253: 743 – 750

el Azzouzi H, Leptidis S, Dirkx E, Hoeks J, van Bree B, Brand K, McClellan EA, Poels E, Sluimer JC, van den Hoogenhof MM, Armand AS, Yin X, Langley S, Bourajjaj M, Olieslagers S, Krishnan J, Vooijs M, Kurihara H, Stubbs A, Pinto YM *et al* (2013) The hypoxia-inducible microRNA cluster miR-199a approximately 214 targets myocardial PPARdelta and impairs mitochondrial fatty acid oxidation. *Cell Metab* 18: 341 – 354

Babar IA, Czochor J, Steinmetz A, Weidhaas JB, Glazer PM, Slack FJ (2011) Inhibition of hypoxia-induced miR-155 radiosensitizes hypoxic lung cancer cells. *Cancer Biol Ther* 12: 908 – 914

Cheng W, Liu T, Wan X, Gao Y, Wang H (2012) MicroRNA-199a targets CD44 to suppress the tumorigenicity and multidrug resistance of ovarian cancer-initiating cells. *FEBS J* 279: 2047 – 2059

Choudhury NR, de Lima Alves F, de Andres-Aguayo L, Graf T, Caceres JF, Rappsilber J, Michlewski G (2013) Tissue-specific control of brain-enriched miR-7 biogenesis. *Genes Dev* 27: 24 – 38

Di Chiro G, DeLaPaz RL, Brooks RA, Sokoloff L, Kornblith PL, Smith BH, Patronas NJ, Kufta CV, Kessler RM, Johnston GS, Manning RG, Wolf AP (1982) Glucose utilization of cerebral gliomas measured by [18F] fluorodeoxyglucose and positron emission tomography. *Neurology* 32: 1323 – 1329

El-Serag HB (2011) Hepatocellular carcinoma. *N Engl J Med* 365: 1118 – 1127

Fischer K, Hoffmann P, Voelkl S, Meidenbauer N, Ammer J, Edinger M, Gottfried E, Schwarz S, Rothe G, Hoves S, Renner K, Timischl B, Mackensen A, Kunz-Schughart L, Andreesen R, Krause SW, Kreutz M (2007) Inhibitory effect of tumor cell-derived lactic acid on human T cells. *Blood* 109: 3812 – 3819

Fong MY, Zhou W, Liu L, Alontaga AY, Chandra M, Ashby J, Chow A, O'Connor ST, Li S, Chin AR, Somlo G, Palomares M, Li Z, Tremblay JR, Tsuyada A, Sun G, Reid MA, Wu X, Swiderski P, Ren X *et al* (2015) Breast-cancer-secreted miR-122 reprograms glucose metabolism in premetastatic niche to promote metastasis. *Nat Cell Biol* 17: 183 – 194

Fukuda T, Yamagata K, Fujiyama S, Matsumoto T, Koshida I, Yoshimura K, Mihara M, Naitou M, Endoh H, Nakamura T, Akimoto C, Yamamoto Y, Katagiri T, Foulds C, Takezawa S, Kitagawa H, Takeyama K, O'Malley BW, Kato S (2007) DEAD-box RNA helicase subunits of the Drosha complex are required for processing of rRNA and a subset of microRNAs. *Nat Cell Biol* 9: 604 – 611

Galban S, Kuwano Y, Pullmann R Jr, Martindale JL, Kim HH, Lal A, Abdelmohsen K, Yang X, Dang Y, Liu JO, Lewis SM, Holcik M, Gorospe M (2008) RNA-binding proteins HuR and PTB promote the translation of hypoxia-inducible factor 1alpha. *Mol Cell Biol* 28: 93 – 107

Garzon R, Marcucci G, Croce CM (2010) Targeting microRNAs in cancer: rationale, strategies and challenges. *Nat Rev Drug Discov* 9: 775 – 789

Guarnieri DJ, DiLeone RJ (2008) MicroRNAs: a new class of gene regulators. *Ann Med* 40: 197 – 208

Guo W, Qiu Z, Wang Z, Wang Q, Tan N, Chen T, Chen Z, Huang S, Gu J, Li J, Yao M, Zhao Y, He X (2015) MiR-199a-5p is negatively associated with malignancies and regulates glycolysis and lactate production by targeting hexokinase 2 in liver cancer. *Hepatology* 62: 1132 – 1144

Hinman MN, Lou H (2008) Diverse molecular functions of Hu proteins. *Cell Mol Life Sci* 65: 3168 – 3181

Hu Y, Liu J, Jiang B, Chen J, Fu Z, Bai F, Jiang J, Tang Z (2014) MiR-199a-5p loss up-regulated DDR1 aggravated colorectal cancer by activating epithelial-to-mesenchymal transition related signaling. *Dig Dis Sci* 59: 2163 – 2172

Jiang S, Zhang LF, Zhang HW, Hu S, Lu MH, Liang S, Li B, Li Y, Li D, Wang ED, Liu MF (2012) A novel miR-155/miR-143 cascade controls glycolysis by regulating hexokinase 2 in breast cancer cells. *EMBO J* 31: 1985 – 1998

Krek A, Grun D, Poy MN, Wolf R, Rosenberg L, Epstein EJ, MacMenamin P, da Piedade I, Gunsalus KC, Stoffel M, Rajewsky N (2005) Combinatorial microRNA target predictions. *Nat Genet* 37: 495 – 500

Kroemer G, Pouyssegur J (2008) Tumor cell metabolism: cancer's Achilles' heel. *Cancer Cell* 13: 472 – 482

Lee YB, Bantounas I, Lee DY, Phylactou L, Caldwell MA, Uney JB (2009) Twist-1 regulates the miR-199a/214 cluster during development. *Nucleic Acids Res* 37: 123 – 128

Lewis BP, Burge CB, Bartel DP (2005) Conserved seed pairing, often flanked by adenosines, indicates that thousands of human genes are microRNA targets. *Cell* 120: 15 – 20

Liu MF, Lu Z, Jiang S, Young KH, Li Y (2010) Physiological and pathological functions of mammalian microRNAs. In *Comprehensive Toxicology: Cellular and Molecular Toxicology*, McQueen CA (ed.), 2nd edn, pp 427 – 446. Oxford: Elsevier Press

Luo W, Semenza GL (2012) Emerging roles of PKM2 in cell metabolism and cancer progression. *Trends Endocrinol Metab* 23: 560 – 566

Majmundar AJ, Wong WJ, Simon MC (2010) Hypoxia-inducible factors and the response to hypoxic stress. *Mol Cell* 40: 294 – 309

Mankoff DA, Eary JF, Link JM, Muzi M, Rajendran JG, Spence AM, Krohn KA (2007) Tumor-specific positron emission tomography imaging in patients: [18F] fluorodeoxyglucose and beyond. *Clin Cancer Res* 13: 3460 – 3469

Masuda K, Abdelmohsen K, Gorospe M (2009) RNA-binding proteins implicated in the hypoxic response. *J Cell Mol Med* 13: 2759 – 2769

Mathupala SP, Ko YH, Pedersen PL (2009) Hexokinase-2 bound to mitochondria: cancer's stygian link to the "Warburg Effect" and a pivotal target for effective therapy. *Semin Cancer Biol* 19: 17 – 24

Mori M, Triboulet R, Mohseni M, Schlegelmilch K, Shrestha K, Camargo FD, Gregory RI (2014) Hippo signaling regulates microprocessor and links cell-density-dependent miRNA biogenesis to cancer. *Cell* 156: 893 – 906

Penna E, Orso F, Cimino D, Tenaglia E, Lembo A, Quaglino E, Poliseno L, Haimovic A, Osella-Abate S, De Pitta C, Pinatel E, Stadler MB, Provero P, Bernengo MG, Osman I, Taverna D (2011) microRNA-214 contributes to melanoma tumour progression through suppression of TFAP2C. *EMBO J* 30: 1990 – 2007

Raimondi L, Amodio N, Di Martino MT, Altomare E, Leotta M, Caracciolo D, Gulla A, Neri A, Taverna S, D'Aquila P, Alessandro R, Giordano A, Tagliaferri P, Tassone P (2014) Targeting of multiple myeloma-related angiogenesis by miR-199a-5p mimics: *in vitro* and *in vivo* anti-tumor activity. *Oncotarget* 5: 3039 – 3054

Ray D, Kazan H, Chan ET, Pena Castillo L, Chaudhry S, Talukder S, Blencowe BJ, Morris Q, Hughes TR (2009) Rapid and systematic analysis of the RNA recognition specificities of RNA-binding proteins. *Nat Biotechnol* 27: 667 – 670

Sakamoto S, Aoki K, Higuchi T, Todaka H, Morisawa K, Tamaki N, Hatano E, Fukushima A, Taniguchi T, Agata Y (2009) The NF90-NF45 complex functions as a negative regulator in the microRNA processing pathway. *Mol Cell Biol* 29: 3754 – 3769

Semenza GL (2010) HIF-1: upstream and downstream of cancer metabolism. *Curr Opin Genet Dev* 20: 51 – 56

Sun S, Ning X, Zhang Y, Lu Y, Nie Y, Han S, Liu L, Du R, Xia L, He L, Fan D (2009) Hypoxia-inducible factor-1alpha induces Twist expression in tubular epithelial cells subjected to hypoxia, leading to epithelial-to-mesenchymal transition. *Kidney Int* 75: 1278 – 1287

Swietach P, Vaughan-Jones RD, Harris AL (2007) Regulation of tumor pH and the role of carbonic anhydrase 9. *Cancer Metastasis Rev* 26: 299 – 310

Tseng JR, Kang KW, Dandekar M, Yaghoubi S, Lee JH, Christensen JG, Muir S, Vincent PW, Michaud NR, Gambhir SS (2008) Preclinical efficacy of the c-Met inhibitor CE-355621 in a U87 MG mouse xenograft model evaluated by 18F-FDG small-animal PET. *J Nucl Med* 49: 129 – 134

Tsukigi M, Bilim V, Yuuki K, Ugolkov A, Naito S, Nagaoka A, Kato T, Motoyama T, Tomita Y (2012) Re-expression of miR-199a suppresses renal cancer cell proliferation and survival by targeting GSK-3beta. *Cancer Lett* 315: 189 – 197

Ueda T, Volinia S, Okumura H, Shimizu M, Taccioli C, Rossi S, Alder H, Liu CG, Oue N, Yasui W, Yoshida K, Sasaki H, Nomura S, Seto Y, Kaminishi M, Calin GA, Croce CM (2010) Relation between microRNA expression and progression and prognosis of gastric cancer: a microRNA expression analysis. *Lancet Oncol* 11: 136 – 146

Vander Heiden MG, Cantley LC, Thompson CB (2009) Understanding the Warburg effect: the metabolic requirements of cell proliferation. *Science* 324: 1029 – 1033

Vander Heiden MG (2011) Targeting cancer metabolism: a therapeutic window opens. *Nat Rev Drug Discov* 10: 671 – 684

Viswanathan SR, Daley GQ, Gregory RI (2008) Selective blockade of microRNA processing by Lin28. *Science* 320: 97 – 100

Wang L, Zhang LF, Wu J, Xu SJ, Xu YY, Li D, Lou JT, Liu MF (2014) IL-1beta-mediated repression of microRNA-101 is crucial for inflammation-promoted lung tumorigenesis. *Cancer Res* 74: 4720 – 4730

Warburg O (1956) On the origin of cancer cells. *Science* 123: 309 – 314

Wiggins JF, Ruffino L, Kelnar K, Omotola M, Patrawala L, Brown D, Bader AG (2010) Development of a lung cancer therapeutic based on the tumor suppressor microRNA-34. *Cancer Res* 70: 5923 – 5930

Wilson WR, Hay MP (2011) Targeting hypoxia in cancer therapy. *Nat Rev Cancer* 11: 393 – 410

Wu L, Belasco JG (2008) Let me count the ways: mechanisms of gene regulation by miRNAs and siRNAs. *Mol Cell* 29: 1 – 7

Yang H, Kong W, He L, Zhao JJ, O'Donnell JD, Wang J, Wenham RM, Coppola D, Kruk PA, Nicosia SV, Cheng JQ (2008) MicroRNA expression profiling in human ovarian cancer: miR-214 induces cell survival and cisplatin resistance by targeting PTEN. *Cancer Res* 68: 425 – 433

Yeligar S, Tsukamoto H, Kalra VK (2009) Ethanol-induced expression of ET-1 and ET-BR in liver sinusoidal endothelial cells and human endothelial cells involves hypoxia-inducible factor-1alpha and microRNA-199. *J Immunol* 183: 5232 – 5243

Zhao S, Gou LT, Zhang M, Zu LD, Hua MM, Hua Y, Shi HJ, Li Y, Li J, Li D, Wang ED, Liu MF (2013) piRNA-triggered MIWI ubiquitination and removal by APC/C in late spermatogenesis. *Dev Cell* 24: 13 – 25